

# Measuring the tip-sample separation in Dynamic Force Microscopy

A. Bugacov<sup>†\*</sup>, R. Resch, C. Baur<sup>‡</sup>, N. Montoya, K. Woronowicz, A. Papson, B. E. Koel,

A. Requicha and P. Will.

*Laboratory for Molecular Robotics, University of Southern California.*

*947 West 37th Place, Los Angeles, CA 90089-0781.*

*E-mail: lmr@lipari.usc.edu.*

*Telephone: +1 (213) 740-4502*

*Fax: +1 (213) 740-7512*

<sup>†</sup> Current address: Dr. Alejandro Bugacov  
USC - Information Sciences Institute  
4676 Admiralty Way, Suite 1001  
Marina del Rey, CA 90292  
E-mail: *bugacov@isi.edu*

<sup>‡</sup> Current address: Dr. Christof Baur  
Zyvex LLC  
1321 North Plano Road, Suite 200  
Richardson, TX 75081  
E-mail: *cbaur@zyvex.com*

## ABSTRACT

We have studied the dependence of the tip-sample separation with the cantilever oscillation amplitude during imaging and manipulation of Au clusters deposited on a functionalized Si substrate. By simultaneously recording the cantilever deflection and oscillation amplitude, as the AFM tip is scanned over a feature with the feedback off, one can elucidate whether the tip was tapping on the substrate or what was the minimum distance between the tip and the substrate. The Si cantilevers that we used presented two different resonance peaks and the experiments show that the selection of the resonance peak has a large influence on the tip-sample separation. When the cantilever is driven close to the high frequency (HF) peak ( $\sim 305$  kHz), the tip oscillates *far* ( $> 4$  nm) from the surface and without contacting it. For driving frequencies close to the low frequency (LF) peak ( $\sim 190$  kHz), the tip oscillates *close* to the surface and taps on the substrate on each oscillation cycle. We find that the tip-sample separation varies linearly with the oscillation amplitude in both cases. In addition, the methods used to calibrate the deflection signal, i.e., convert from volts to nanometers, are discussed in detail. Knowledge of the actual distance between tip and sample can play an important role in improving nanomanipulation with an SPM. For example, the tip can be lowered and be positioned at the optimal height for manipulation without risk of crashing into the sample.

Keywords: Nanomanipulation, Scanning Probe Microscopy, Nanotechnology, Nanostructures, Nanoparticles.

Abbreviated Title: Measuring the tip-sample separation

## 1. INTRODUCTION

In recent years the Atomic Force Microscope (AFM) [Binnig et al. (1986)] has become an extremely valuable scientific tool due to its versatility and capability both in ambient and liquid environments. In particular, when the AFM is operated in dynamic mode (DFM) [Martin et al. (1987), Lüthi et al. (1994)], topographic images can be obtained with almost no damage to the sample. This feature is very attractive for the investigation of "soft" samples like the ones usually found in biology and surface science [Anselmetti et al. (1994)]. Furthermore, the AFM has transcended its main purpose of analyzing surface topography and found applications in different fields like Nano-manipulation [Junno et al. (1995)-(1997), Schaefer et al. (1995), Baur et al. (1997)-(1998), Resch et al. (1998a)-(1998b)] and Atomic Force Spectroscopy [Spatz et al. (1995), Anczykowski et al. (1996), Sarid et al. (1996), Tamayo and García (1996), Kühle et al. (1997), Burnham et al. (1997)].

When imaging in DFM, the cantilever is driven by the sinusoidal excitation of a piezoelectric material in mechanical contact with its base and the feedback system adjusts the  $z$  position of the scanner (i.e.; the tip-sample separation) to keep the amplitude  $A$  of the oscillating free end of the cantilever equal to the selected or setpoint value  $A_{set}$ . However, the absolute distance between the tip and the substrate is not known and, especially when working in ambient conditions, this value can be very difficult to estimate from first principles. Unless some detail investigation procedure has been conducted for each specific tip-sample system, the user does not have *a priori*

information of whether the tip is intermittently contacting (*tapping*) the surface during each oscillation cycle or oscillating without reaching the sample. Therefore, by DFM we refer both to *tapping* and *non-contact* modes of operations where only the oscillation amplitude of the cantilever is used to control the instrument. In the type of AFM nanomanipulation discussed here, the tip of the cantilever is used to *push* a nanoparticle to its desired new location. Knowledge of the tip-particle separation may provide additional control over current manipulation strategies [Resch et al. (1998)] and enable the manipulation of smaller objects.

We present an experimental procedure that allows us to estimate the distance between the tip and the substrate during normal imaging conditions. This scheme consists of measuring, simultaneously, the cantilever d.c.-deflection and change in oscillating amplitude while the tip is scanned over a nanometer-size particle *with the feedback off*.

## 2. EXPERIMENTAL PROCEDURES

The samples were prepared by depositing 15 to 30 nm gold colloidal particles (EM.GC15; Ted Pella Inc.) from aqueous solution on Si substrates that had been previously functionalized by a monolayer of APTS [N-(2-Aminoethyl) 3-Aminopropyl-Trimethoxysilane].

The experiments were carried out with an AutoProbe CP<sup>®</sup> AFM (Park Scientific Instruments) operated in dynamic mode (DM-AFM) in air and at room temperature. We used commercially-available triangularly-shaped silicon cantilevers (Park Scientific

Instruments) with integrated conical tips. There are four cantilevers (A-D) on each Si chip, but throughout these experiments we always used the cantilever "C" which has a spring constant of about 13.0 N/m (according to the nominal value supplied by the vendor).

The following measuring procedure was used throughout the experiments. First, we select appropriate values of the driving frequency,  $f_{dr}$ , and the driving amplitude,  $A_{free}$ , and image the sample in dynamic mode. Then, utilizing the Probe Control Software (PCS) developed by our group [Baur et al. (1997)], the user draws an arrow with the mouse over the image, and performs a single-line scan along the arrow. In the experiments reported here, the scan trajectories were held at the center of the selected particle by a tracking system that continuously repositions the scan line (without adjusting its direction) to maximize the feature height. The tracking system ensures that every line-scan is done in the same position relative to the sample frame of reference and thus compensates for drift. The user also sets two points along the specified trajectory, such that the feedback is turned off at the first point and re-engaged at the second point. We selected these two points to be before and after the particle.

We started a series of measurements by selecting the largest  $A_{set}$  for which imaging was possible. While imaging (i.e., with the feedback on), we measured the cantilever oscillation amplitude  $A_{set}$ . In a subsequent scan, we disabled the feedback between the two marks and recorded the cantilever d.c.-deflection,  $D_{dc}$ , and the change in the oscillation amplitude,  $\Delta A$ , during that part of the scan. Then, we decreased the setpoint

and repeated the procedure. To avoid crashing the tip into the surface, we stopped decreasing  $A_{set}$  either when imaging conditions were no longer stable or when the particle moved.

## 2.1 Selection Of The Driving Frequency

Most of the cantilevers used in the experiments had a *free* frequency response like the one showed in Figure 1. Two peaks can be distinguished in the figure. A weak, low frequency (LF) peak occurred at  $f_{LF} \sim 190$  kHz and a strong, high frequency (HF) peak was found at  $f_{HF} \sim 305$  kHz. The presence of multiple peaks may be attributed to the triangular shape of the cantilevers and/or to the additional mechanical complexity introduced by mounting the cantilever chip on the instrument.

We drove the cantilevers at the frequency  $f_{dr}$  and free amplitude  $A_{free}$  that produced stable imaging conditions. We selected  $f_{dr}$  either near the LF ( $f_{dr} \sim f_{LF}$ ) or the HF peak ( $f_{dr} \sim f_{HF}$ ). Values of  $f_{dr}$  both to the right or the left of the local maximum were tested. In these experiments,  $5 \text{ nm} < A_{free} < 10 \text{ nm}$  for  $f_{dr} \sim f_{LF}$  and  $10 \text{ nm} < A_{free} < 16 \text{ nm}$  for  $f_{dr} \sim f_{HF}$ .

## 2.2 Volts-to-Nanometers Calibration Of The Deflection Signal

Special consideration should be given to the fact that  $A_{set}$ ,  $D_{dc}$  and  $\Delta A$  are all measured in Volts by analyzing, using an oscilloscope, the differential (A-B) signal

coming from the split photocell of the microscope's beam deflection system. Therefore, in order to convert these quantities to units of length (nm), the photocell must be calibrated. We have found that this calibration factor varied significantly for different sessions where different cantilevers and photocell positions were used. Therefore, *an independent calibration of the photocell was performed for each session*. Our observations indicate that this necessity is mainly due to the fact that in our instrument the A-B photocell signal is not normalized to the total (A+B) photocell signal. Geometric factors may also influence the calibration.

We used two different calibration procedures. First we selected a scan trajectory that passed through the center of two particles of different heights. In this case, the difference in  $D_{dc}$  should correspond to the difference in height (which we know from the topographic signal). This procedure does not change the shape of the tip and can be performed using the PCS during the manipulation session. Secondly, we switched to contact-mode, disabled the feedback, and recorded the change of  $D_{dc}$  as we changed the  $z$ -position of the scanner by small increments ( $\sim 1\text{nm}$ ). This procedure may cause deterioration in the shape of the tip, and so it was performed only at the end of each experimental session.

To maintain the value of (A+B) constant and to minimize the effect of geometric factors, both calibration procedures were done during the same experimental session and without modifying the setup or changing the position of the photocell relative to the cantilever. The first calibration method is performed in DFM, i.e., the tip is being driven

and the value of  $D_{dc}$  is extracted from the d.c. component of the (A-B) photocell signal. It must be noted that for the part of the scan for which  $D_{dc} > 0$  (see Figure 2b), the oscillation amplitude of the cantilever is totally damped (i.e.,  $A \sim 0$ ) (see Figure 3 and [Resch et al. (1998)]) and effects due to the variation of the photo-detector response with frequency cannot be important. During the second calibration procedure, the cantilever was not driven, the tip was carefully brought to contact with the surface and the change of the d.c. component of the (A-B) signal was recorded as the  $z$ -position of the scanner was changed by known amounts.

For the results presented in the following section, the calibration factors varied from 38 to 43 nm/V. The values obtained by the two independent methods, described above, agreed to within 15%. Another way of checking the consistency of the calibration is to consider that in the limit of  $A_{set} \rightarrow 0$ , the tip is close enough to the surface that the corresponding d.c.-deflection must be nearly equal to the height of the particle. We show later in Figure 3b that this third criterion for estimating a calibration factor is satisfied to within 10%.

### 3. RESULTS

In DFM, the cantilever is driven by a sinusoidal excitation of its base but its dynamic state is ultimately determined by the non-linear interaction of the tip with the substrate. Our analysis of the photocell differential signal (A-B) during imaging with cantilevers with  $k_c \sim 13$  N/m agrees with conclusions from experiments and computer simulations

[Sarid et al. (1996), Burnham et al. (1997), Resch et al. (1998), Cleveland et al. (1998), Whangbo et al. (1998), García et al. (1998), Tamayo and García (1998)] that the dynamic state of the cantilever remains highly sinusoidal in spite of the presence of non-linear interaction forces. In Figure 2, we show our *picture* of the interaction of the oscillating tip with the nanoparticle while the feedback is off, which is based on this assumption and the interpretation of our data and previous numerical simulations [Resch et al. (1998)]. Two different situations are illustrated. For large values of the setpoint, as shown in Figure 2a, the separation  $S_0$  between the oscillation average position and the substrate is larger than the height  $H$  of the particle and the tip can *pass over* the feature without undergoing a detectable d.c.-deflection. The main result of the tip-particle interaction is to decrease the oscillation amplitude. The opposite situation, for which  $S_0 < H$ , is sketched in Figure 2b. In this case, as a result of the interaction with the particle, the cantilever oscillation amplitude gets totally damped and a net d.c.-deflection of the cantilever occurs.

Based on this model, we measured the maximum cantilever d.c.-deflection,  $D_{max}$ , and the drop in the oscillation amplitude,  $\Delta A = A_{set} - A_{min}$ , during a single line-scan passing through the center of a nanoparticle.  $A_{min}$  denotes the minimum value of the amplitude during the line-scan. The height,  $H$ , of the particles was in the range of 20 to 24 nm. In Figure 3a, we show the normalized amplitude drop,  $\Delta A/H$ , as a function of the normalized setpoint,  $A_{set}/H$ . Each curve corresponds to a different particle and not all of them were obtained using the same cantilever. The cantilevers were driven near the HF peak with  $f_{dr} \sim f_{HF} \cong 305$  KHz and with a free oscillation amplitude of 10 - 16 nm. Driving frequencies both to the right and to the left of the resonant frequency were

selected. Again, the particles did not move during the measurements. All of the curves in Figure 3a show a similar behavior. For large values of  $A_{set}$  (see Figure 2a), the normalized amplitude drop stays nearly constant at a value of about 0.25. This indicates that the tip apex, while in the imaging mode, is far from reaching or *tapping* the surface. Otherwise, the normalized drop in amplitude should be close to 1.0. As we decreased the setpoint,  $\Delta A$  decreased and became equal to  $A_{set}$ . This is shown in Figure 3a by a nearly straight line with a slope of unity for values of  $A_{set}/H$  smaller than  $\sim 0.25$ . These results correspond to the situation depicted in Figure 2b where the oscillation amplitude gets totally damped as a result of the tip-particle interaction.

In Figure 3b we plot the corresponding values of the normalized maximum deflection,  $D_{max}/H$ , as a function of the normalized setpoint. As seen in this figure,  $D_{max} \sim 0$  for setpoint values where  $\Delta A$  is constant. This is consistent with the picture given in Figure 2a. As  $A_{set}$  is decreased, the average  $z$ -position of the tip moves below the height  $H$  of the particle and  $D_{max}$  becomes larger than zero. This means that when the tip is on top of the particle, it is deflected an amount  $D_{max}$  relative to its previous average  $z$ -position. This situation corresponds to the one sketched in Figure 2b. As seen in comparing Figs. 3a and b,  $\Delta A \cong A_{set}$  for these setpoint values and therefore the oscillation amplitude is nearly zero during the interaction of the tip with the particle.

Because the cantilever oscillation is totally damped and a d.c.-deflection of the cantilever occurs, we conclude that the tip must be in continuous contact with the particle for the part of the scan during which these two conditions are satisfied. In Figure 3b the

onset of deflection occurs at  $A/H \sim 0.25$  for all curves. The scaling of both the onset of deflection and the inflection of the  $\Delta A$  curves with the height of the particle is a consequence of the linear dependence of the mean tip-sample separation with the setpoint (This will be shown clearly later in Figure 4). Importantly, extrapolation of the curves shown in Figure 3b, give intersections with the y-axis at  $D_{max}/H \sim 1$ . This means that in the limit of  $A_{set} \rightarrow 0$  the tip deflected the entire height of the particle and provides an independent way of checking the consistency of the volts-to-nanometer calibration.

Now we focus on the problem of estimating the separation between the tip and the sample during experiments using the AFM in dynamic mode. From Figure 2, the mean tip-sample separation  $S_0$  can be written as:

$$S_0 = \begin{cases} H - D_{max} & \text{if } D_{max} > 0 \\ H + S_P + (A_{set} - \Delta A) & \text{if } D_{max} \approx 0 \end{cases} \quad (1)$$

$$(2)$$

Assuming that the motion of the cantilever remains highly sinusoidal during the experiments [Burnham et al. (1997), Tamayo and García (1998), Resch et al. (1998), Cleveland et al. (1998), Whangbo et al. (1998)], the minimum tip-sample separation,  $S_s$ , can be calculated as  $S_s = S_0 - A_{set}$  if  $S_0$  is known. In Figure 4 we plot the values of  $S_0$  (■) and  $S_s$  (●) calculated from Eq. 1 corresponding to the data sets shown in Figure 3 (driving frequencies near the HF peak) and the values of  $S_0$  (□) and  $S_s$  (○) corresponding

to driving frequencies near the LF resonant peak. Since we cannot measure  $S_p$ , we have plotted  $S_0$  and  $S_s$  only for those values of  $A_{set}$  for which  $D_{max} > 0$  was detected. In order to estimate  $S_p$ , we have extrapolated  $S_0$  for values of  $A_{set}$  for which  $D_{max} \approx 0$  following the trend marked on the HF curve (■) and plotted the values of  $S_p$  (▲) calculated from Eq. 2. The height of the particles,  $H$ , ranged from 20 to 24 nm. The lowest data point plotted on the LF curve corresponded to the smallest value of  $A_{set}$  that did not move the particles. In the HF case, the particles did not move regardless of the value of the setpoint. As seen in Figure 4, the mean tip-sample separation  $S_0$  varies linearly with the cantilever oscillation amplitude  $A_{set}$  both for driving frequencies near the LF or the HF peak. However, the values of  $S_0$  and the slopes of the curves are quite different in each case. For  $f_{dr} \sim f_{HF}$ , the slope of the curve is approximately 3.8 and we see that the tip oscillates relatively *far* from the surface ( $S_0 > 4$  nm) and does not contact it. In the case of  $f_{dr} \sim f_{LF}$ , the slope of the curve is nearly 1.0, as would be the case if the tip were tapping on the surface during each oscillation, i.e.,  $S_0 \cong A_{set}$ .

For setpoint values producing no d.c.-deflection ( $A_{set} > 5$  nm), we see that the estimated values of the minimum tip-particle distance  $S_p$  (HF) ranges from 0 - 15 nm. This curve has the same slope as the  $S_s$  curve because the amplitude drop  $\Delta A$  is nearly constant for those values of  $A_{set}$ , as was shown in Figure 2a.

The results of Figure 4 indicate that for a given value of  $A_{set}$ , the tip oscillates much closer to the surface when driven at a frequency near the LF peak than near the HF peak. Within the harmonic approximation [Martin et al. (1987), Whangbo et al. (1998)], this

may indicate that the  $Q$  of the LF resonance is smaller than that of the HF peak and so the cantilever must get closer to the surface to produce a similar amount of damping of the oscillation amplitude.

Looking back at Eq. 1, we can also say that  $D_{max}$  is larger for the LF than for the HF case for the same value of  $A_{set}$ . This has a direct influence on manipulating nanoparticles. As we have previously reported [Resch et al. (1998)], there is a threshold in the d.c.-deflection for the onset of manipulation for a given combination of particle size, substrate and value of the cantilever spring constant. From Eq. 1 we have that  $D_{max} = H - S_0$  and the threshold can then be written as  $D_{TH} = H - S_0^{Min}$ , where  $S_0^{Min}$  is the lowest value of  $S_0$  for which the particle did not move. By looking at the LF curve of  $S_0$  ( $\square$ ) in Figure 4 we see that  $S_0^{Min} \cong 2$  nm. Then, by using the average particle height  $H = 22$  nm we obtain  $D_{TH} = H - 2$  nm = 20 nm for the estimate value of the threshold. In Figure 3b we have that  $D_{max}/H < 0.8$  for all values of  $A_{set}$ . Using the maximum particle height  $H = 24$  nm, this corresponds to  $D_{max} < 19.2$  nm and explains why the particles were never moved when the cantilever was driven near the HF peak.

#### 4. CONCLUSIONS

We described an experimental procedure to estimate the *absolute* separation between the tip and sample during operation of an AFM in dynamic mode. This method does not involve ramping of the scanner in the  $z$ -direction, and therefore the risk of damaging the tip during these measurements is no higher than under normal operating conditions. The Si cantilevers that we used were characterized by two main resonant frequencies ( $f_{LF} \sim$

190 kHz and  $f_{HF} \sim 305$  kHz) and the results differed significantly depending on whether the cantilever was driven near the low or high frequency peak. When the driving frequency was close to  $f_{LF}$ , the average tip-sample separation was nearly equal to the oscillation amplitude and the tip tapped on the surface during each oscillation cycle. When the cantilever was driven close to the high frequency peak, the average tip-sample separation also varied linearly with  $A_{set}$  but with a slope of  $\sim 3.8$  and the tip oscillated without contacting the surface. Driving the cantilever to the left or the right of each resonant frequency did not influence these results.

In addition, we provided a detailed description of methods used to calibrate the photocell signal, i.e., to convert the values of the cantilever deflection (and oscillation amplitude) from volts to nanometers. We found the calibration to be very sensitive to the experimental setup and so we recommend that the photocell be calibrated for each session in order to obtain meaningful results.

The results presented here have important implications in improving nano-manipulation with an AFM by showing strategies to increase reliability and manipulate smaller particles (e.g., below 5 nm). Because we can interactively estimate the distance between the tip and the sample, the tip can be lowered to a position at the optimal height for manipulation without risk of crashing the tip into the sample.

## 5. ACKNOWLEDGMENTS

We thank Dr. R. García and the referees for helpful comments on the text. This research was supported by the Z. A. Kaprielian Technology Innovation Fund.

## 6. REFERENCES

- Anczykowski, B., Kruger, D., Fuchs, H. (1996). Cantilever dynamics in quasinoncontact force microscopy: spectroscopic aspects. *Physics Review B* 53 15485-15488.
- Anselmetti, D., Lüthi, R., Meyer, E., Richmond, T., Dreier, T., Frommer, J.E. and Güntherodt, H. J. (1994), Attractive-Mode Imaging of Biological Materials with Dynamic Force Microscopy, *Nanotechnology* 5, 87.
- Baur, C., Bugacov, A., Koel, B. E., Madhukar, A., Montoya, N., Ramachandran, T. R., Requicha, A. A. G., Resch, R. and Will, P. (1998), Nanoparticle manipulation by mechanical pushing: underlying phenomena and real-time monitoring, *Nanotechnology*, in press.
- Baur, C., Gazen, B. C., Koel, B. E., Ramachandran, T. R., Requicha A. A. G. and Zini, L. (1997), Robotic nanomanipulation with a scanning probe microscope in a networked computing environment, *Journal of Vacuum Science and Technology B* 15, 1577-1580.
- Binnig, G., Quate, C. F. and Gerber, Ch. (1986). Atomic Force Microscope, *Physical Review Letters* 56, 930 - 933.
- Burnham, N. A., Behrend, O. P., Oulevey, F., Gremaud, G., Gallo, P. J., Gourdon, D., Dupas, E., Kulik, A. J., Pollock, H. M. and Briggs, G. A. D. (1997), How does a tip tap?, *Nanotechnology* 8, 67-75.
- Cleveland, J. P., Anczykowski, B., Schmid, A. E., Elings, V. B. (1998), Energy-dissipation in tapping-mode atomic-force microscopy, *Applied Physics Letters* 72, 2613.
- D.M. Schaefer, R. Reifenberger, A. Patil, and R.P. Andres, *Appl. Phys. Lett.* 66, 1012 (1995).
- García, R., Calleja, M., and Pérez-Murano, F. (1998), Local oxidation of silicon surfaces by dynamic force microscopy: nanofabrication and water bridge formation, *Applied Physics Letters* 72, 2295.
- Junno, T., Carlsson, S. B., Xu, H., Montelius, L. and Samuelson, L. (1997), Fabrication of quantum devices by angstrom-level manipulation of nanoparticles with an atomic-force microscope, *Applied Physics Letters* 72, 548.
- Junno, T., Deppert, K., Montelius, L. and Samuelson, L. (1995), Controlled manipulation of nanoparticles with an atomic force microscope, *Applied Physics*

Letters 66, 3627-3629.

- Kühle, A., Sorensen, A. H., Bohr, J. (1997), Role of attractive forces in tapping tip force microscopy, *Journal of Applied Physics* 81, 6562-6569.
- Lüthi, R., Meyer, E., Howald, L., Haefke, H., Anselmetti, D., Dreier, M., Rüetschi, M., Bonner, T., Overney, R. M., Frommer, J., and Güntherodt, J. H. (1994), Progress in non-contact dynamic force microscopy, *Journal of Vacuum Science and Technology B* 12, 1673.
- Martin, Y., Williams, C. C. and Wickramasinghe, H. K. (1987), Atomic force microscope-force mapping and profiling on a sub 100 Å scale, *Journal of Applied Physics* 61, 4723 - 4729.
- Resch, R., Baur, C., Bugacov, A., Koel, B. E., Madhukar, A., Requicha, A. A. G. and Will, P. (1998), Building and manipulating 3-D and linked 2-D structures of nanoparticles using scanning force microscopy, *Langmuir*, in press.
- Resch, R., Bugacov, A., Baur, C., Koel, B. E., Madhukar, A., Requicha A. A. G. and Will, P. (1998), Manipulation of nanoparticles using dynamic force microscopy: simulation and experiments, *Applied Physics A* 67, 265.
- Sarid, D., Ruskell, T. G., Workman, R. K., Chen, D. (1996), Driven nonlinear atomic-force microscopy cantilevers: from noncontact to tapping modes of operation, *Journal of Vacuum Science and Technology B* 14, 864-867.
- Schaefer, D. M., Reifengerger, R., Patil, A. and Andres, R. P. (1995), Fabrication of two-dimensional arrays of nanometer-size clusters with the atomic force microscope, *Applied Physics Letters* 66, 1012-1014.
- Spatz, J. P., Sheiko, S., Moller, M., Winkler, R. G., Reineker, P., Marti, O. (1995), Forces affecting the substrate in resonant tapping force microscopy, *Nanotechnology* 6, 40-44.
- Tamayo, J., Garcia, R. (1996), Deformation, contact time, and phase-contrast in tapping mode scanning force microscopy, *Langmuir* 12 4430-4435.
- Tamayo, J, Garcia, R (1998), Relationship between phase-shift and energy-dissipation in tapping-mode scanning force microscopy, *Applied Physics Letter* 73, 2926-2928.
- Whangbo, M. -H, Bar, G., Brandsch, R. (1998), Description of phase imaging in tapping mode atomic-force microscopy by harmonic approximation, *Surface Science* 411, 1794-1801.

## 7. FIGURE CAPTIONS

Figure 1: Typical frequency response of Si cantilevers used throughout these experiments.

Figure 2: Sketch of the dynamic state of the cantilever during the interaction of the AFM tip with a particle on a flat support. (a) For high setpoint values the amplitude  $A$  is reduced but no d.c.-deflection occurs. (b) For low setpoint values the amplitude becomes totally damped and the cantilever undergoes a d.c.-deflection.

Figure 3: Dependence of the normalized drop in the cantilever amplitude signal during a scan,  $\Delta A/H$ , (a) and normalized maximum cantilever deflection  $D_{max}/H$ , (b) with the normalized setpoint value,  $A_{set}/H$ . Results are shown for cantilever driving frequencies near the HF resonance peak. The particle heights,  $H$ , ranged from 20 - 24 nm.

Figure 4: Dependence of the tip-sample separation with the cantilever oscillation amplitude  $A_{set}$ . Results are shown for the average tip-sample separation  $S_0$  with driving frequencies near the HF (■) and the LF (□) resonance peak, the minimum tip-sample separation  $S_s$  with driving frequencies near the HF (●) and the LF (○) resonance peak, and the minimum tip-particle separation  $S_p$  (▲) for cantilevers driven near the HF peak.

Figure 1

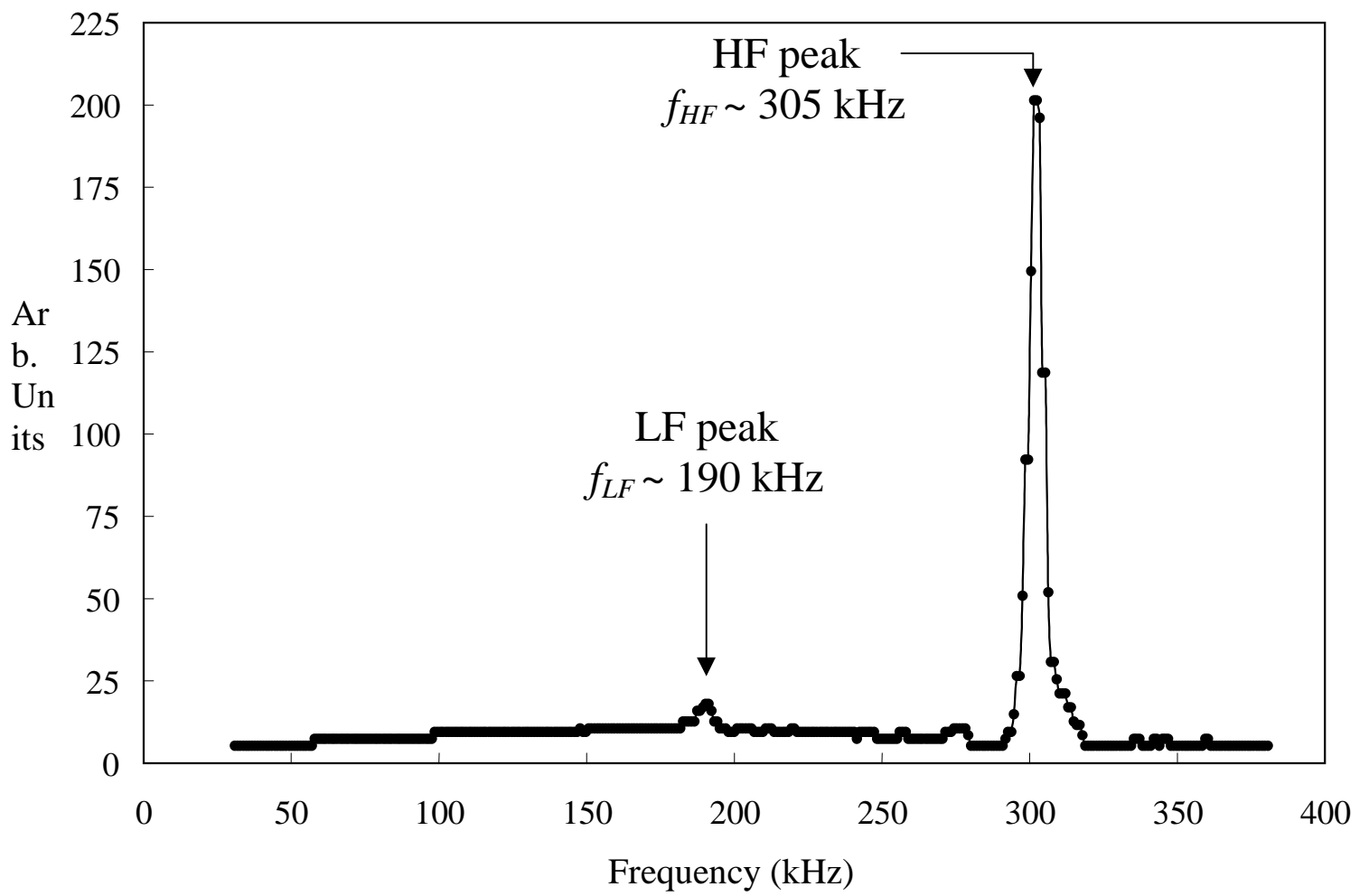


Figure 2

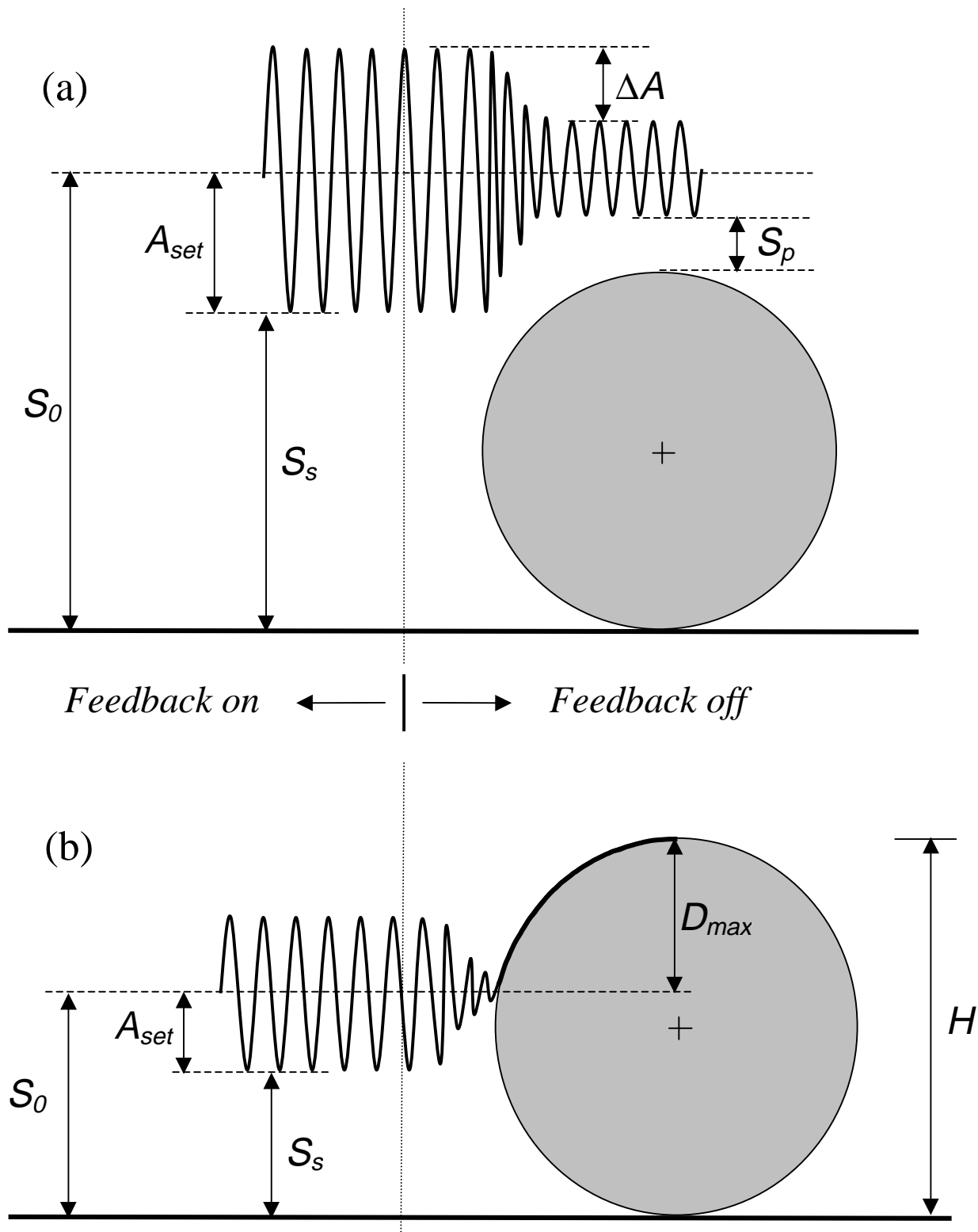


Figure 3

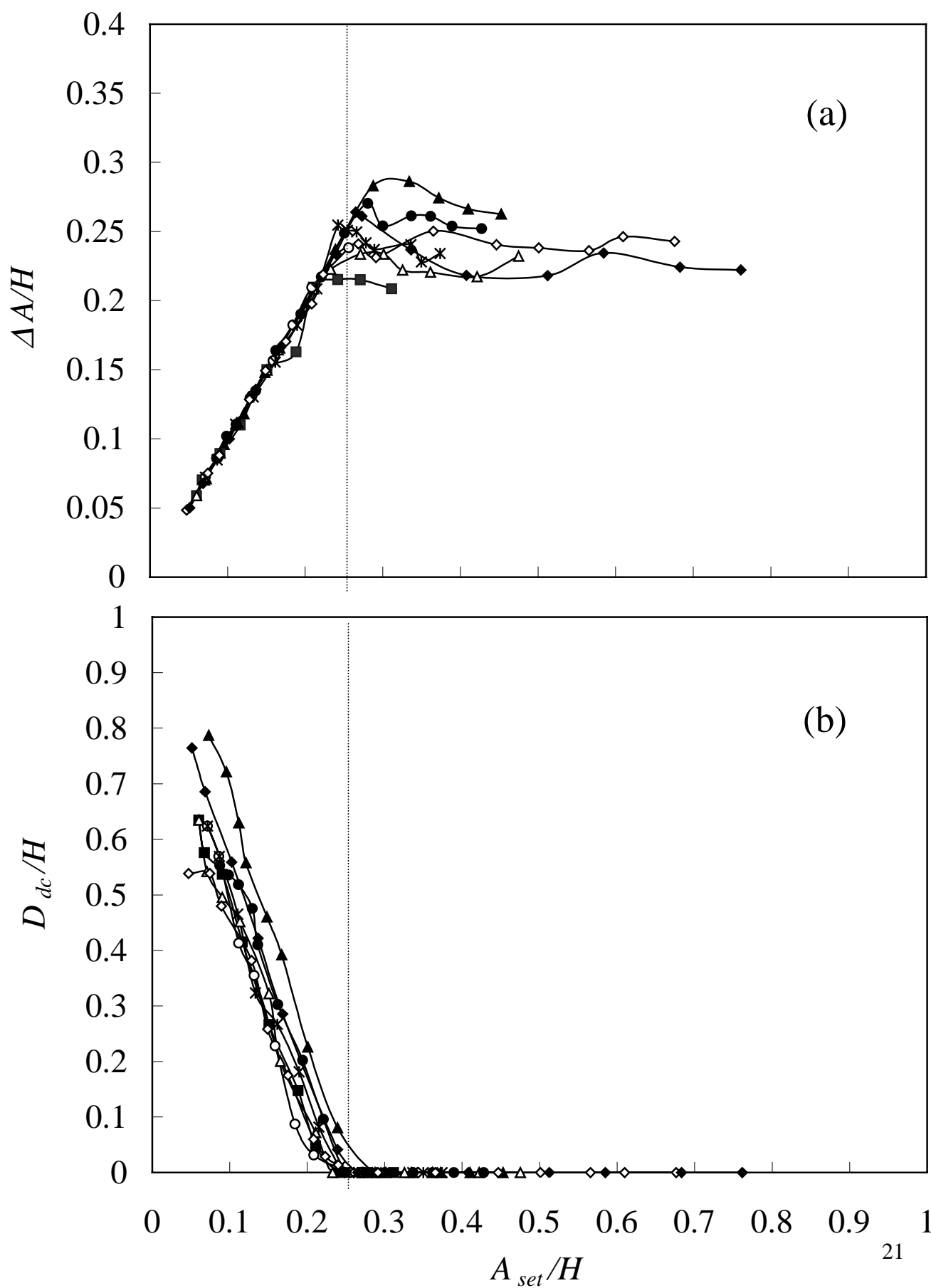


Figure 4

